

High Performance Thermoelectric Materials Based on Metal Organic Coordination Polymers through First-Principles Band Engineering

Jahanzeb Khan^{1b},^{†[a]} Yunpeng Liu,^{†[a]} Tianqi Zhao,^[a] Hua Geng^{1b},^{*[b]} Wei Xu,^[c] and Zhigang Shuai^{*[a]}

Metal organic coordination polymers (MOCPs) provide an intriguing platform to design functional thermoelectric materials through modifying metal atoms, organic ligands, etc. Based on density functional theory (DFT) coupled with Boltzmann transport theory, the thermoelectric properties of several MOCPs, which is designed by intercalating organic linkers ranging from benzene to pentacene between two inorganic units, have been investigated. We found that the interplay of d orbital of Ni atom

and π orbitals of the organic linkers play an important role in band engineering and then thermoelectric efficiency. Combining the high conductivity for π orbitals of organic ligands and high Seebeck coefficient of the d orbital of Ni atom, such intercalated MOCPs provide new way to design high performance thermoelectric materials. © 2018 Wiley Periodicals, Inc.

DOI:10.1002/jcc.25639

Introduction

Motivated by the rapid growing global demand in energy, highly efficient thermoelectric (TE) materials have attracted great attentions in recent decades.^[1–5] Organic thermoelectric (OTE) materials have received increasing research interests due to their intrinsically low thermal conductivity, low cost, low weight, environment friendly, and elements abundance.^[6–12] For p-type transport Poly(3,4-ethylenedioxythiophene; PEDOT) blended with poly(styrenesulfonate) (PSS) has been shown the highest dimensionless figure of merit zT up to 0.42. Nevertheless, very few n-type OTE materials have been reported yet, as low electrical conductivity is detrimental to their TE efficiency.^[13–17] The effectiveness of TE materials is measured by a dimensionless figure of merit as zT :

$$zT = \frac{S^2 \sigma T}{\kappa_e + \kappa_l} \quad (1)$$

where S is the Seebeck coefficient, σ is electrical conductivity, $S^2 \sigma$ is power factor, T is the average temperature, and κ is thermal conductivity for electrons and lattice. It is highly challenging, to boost this promising green power generation technology by enhancing the figure of merit zT of current organic TE materials.^[2,12,18] However, it is knotty to enhance the zT value in a straightforward way as all these parameters are strongly interdependent with each other.^[5,19] To obtain a highly efficient TE material, it is required to lower thermal conductivity, to increase electrical conductivity, and to enhance Seebeck coefficient, respectively.^[20,21]

Metal organic coordination polymers (MOCPs), formed by transition metal ions and organic ligand are ladder-like polymers; the absence of rotatable single-bond connections makes the polymer chain highly rigid, as a result facilitates the extension of the charge conjugation through the polymer back-bone and the intrachain charge transport is expected to be highly

efficient. To the best of our knowledge, Poly[K_x (Ni-ett)] formed by the metal Ni atom and ethylene ligand have been found to possess the highest efficiency for n-type organic thermoelectric materials with power factor of $453 \mu\text{Wm}^{-1} \text{K}^{-2}$ at 300 K ever reported to date.^[21] Poly(Na_2 Ni-ett) also revealed good n-type TE properties due to high electrical conductivity and maximum power factor up to $27.62 \mu\text{Wm}^{-1} \text{K}^{-2}$ at room temperature has been achieved.^[22,23] Similar conducting polymers, by modifications in organic moieties and inorganic metal ions have been synthesized and investigated right after and to improve the carrier density and electrical conductivity, the doping with counter cations, that is, K^+ and Na^+ have been generally introduced.^[24–30] Since, high carrier concentration and charge mobility are destructive to Seebeck coefficient (S). Conversely, in MOCPs the combination of localized d-orbital of Metal atom and delocalized π orbitals of organic ligands will probably provide high conductivity and large Seebeck coefficient simultaneously.

[a] J. Khan¹, Y. Liu¹, T. Zhao, Z. Shuai
MOE Key Laboratory of Organic Optoelectronics and Molecular Engineering,
Department of Chemistry, Tsinghua University, Beijing 100084, China
E-mail: zgshuai@tsinghua.edu.cn

[b] H. Geng
Department of Chemistry, Capital Normal University, Beijing 100048, China
E-mail: hgeng@cnu.edu.cn

[c] W. Xu
Beijing National Laboratory for Molecular Sciences, CAS Key Laboratory of
Organic Solids, Institute of Chemistry, Chinese Academy of Sciences, Beijing
100190, China

[†]These authors contributed equally to this work.

Contract Grant sponsor: National Natural Science Foundation China;
Contract Grant numbers: 21788102, 21673247; Contract Grant sponsor:
National Key R&D Program of China; Contract Grant number:
2017YFA0204700; Contract Grant sponsor: Beijing Capacity Building for
Sci-Tech Innovation-Fundamental Scientific Research Funds; Contract
Grant number: 025185305000; Contract Grant sponsor: Strategic Priority
Research Program of the Chinese Academy of Sciences; Contract Grant
number: XDB12020200

© 2018 Wiley Periodicals, Inc.

Band engineering based on molecular design has been found an effective methodology to enhance zT of TE materials.^[31–35] As the physical properties (i.e., electronic bandgap, bandwidth) of MOCPs are tunable by varying the composition of the organic bridging linker. By insertion of organic linkers of various lengths between two inorganic units, we can modulate TE efficiency through band engineering. Herein, we report a series of MOCPs, Poly(A₂Ni-Y-ts) (as Scheme 1) containing (A = Na, Y = ethylene, benzene, naphthalene, anthracene, tetracene, and pentacene, respectively, and ts = tetraselenolate), (Ethylene-tetraselenolate = ets, Benzene-tetraselenolate = bts, Naphthalene-tetraselenolate = nts, Anthracene-tetraselenolate = ats, Tetracene-tetraselenolate = tts, and Pentacene-tetraselenolate = pts) and investigated their TE properties. Based on Boltzmann theory coupled with deformation potential theory at the first-principles level, we found that Poly(Na_xNi-ets) reveals the best N-type TE properties, the maximum power factor for Poly(Ni-ets) is achieved up to 470 $\mu\text{Wm}^{-1} \text{K}^{-2}$ at room temperature, which is comparable with the power factor (453 $\mu\text{Wm}^{-1} \text{K}^{-2}$) for Poly(K_xNi-ett).^[21] Through introduction of different organic ligands of varied chain lengths, the TE efficiency can be modulated due to band structure engineering.

Computational and Methodological Approaches

The geometric and electronic band structure calculations were done under the density functional theory (DFT), by using projected augmented wave (PAW) method as executed in the Vienna Ab initio Simulation Package (VASP, version 5.3.2).^[35,36] The Perdew–Burke–Ernzerhof (PBE)^[37] exchange correlation functional was adopted for optimization. For the optimization of the

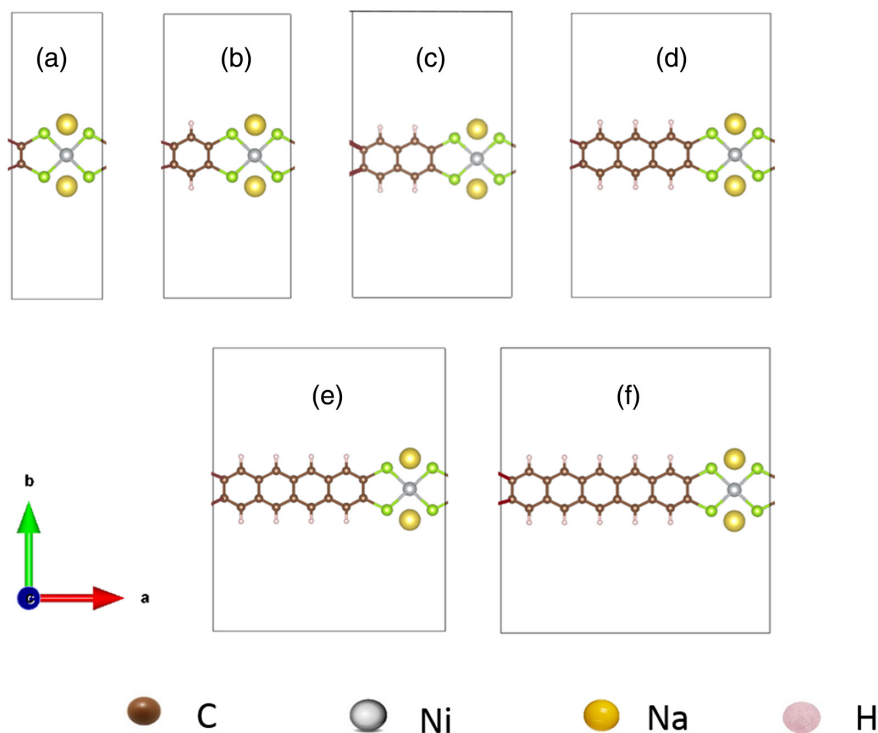
lattice parameters and atomic positions, $4 \times 1 \times 1$ Monkhorst–Pack^[38] \mathbf{k} -mesh was used until the forces were relaxed within 0.01 eV/Å on each atom. The criterion in the self-consistent field iteration for total energy convergence was fixed to 10^{-5} eV and the kinetic energy cutoff was set to be 600 eV. The hybrid functional (HSE-06)^[39] exchange correlation functional was adopted for SCF, band structure and densities of states DOS calculations. For the convergence of charge density, $8 \times 1 \times 1$ Monkhorst–Pack \mathbf{k} -mesh was adopted, while denser Monkhorst–Pack \mathbf{k} -mesh $21 \times 1 \times 1$ was used to calculate transport coefficients. With respect to highly oriented polymer chain, band transport mechanism dominates due to strong intrachain electronic delocalization. Under the relaxation time approximation, Seebeck coefficient S and electrical conductivity σ can be obtained by solving the steady-state Boltzmann transport equation and using BoltTraP code.^[40]

Boltzmann transport theory

The Boltzmann transport equation (BTE) is used to get the thermoelectric properties in our calculation. The electronic distribution follows the Fermi–Dirac Distribution when no external field presents.

$$f_0(\varepsilon_{\mathbf{k}}) = \frac{1}{\exp[(\varepsilon_{\mathbf{k}} - \varepsilon_f)/k_B T] + 1} \quad (2)$$

Where ε_f is the Fermi level, and $\varepsilon_{\mathbf{k}}$ is the electronic band energy at a given \mathbf{k} -point, k_B is Boltzmann constant, and T is the temperature.^[17] Under the external fields and at steady-state including the electric or magnetic fields and thermal gradient, the distribution function in the phase space $f(\mathbf{r}, \mathbf{k}, t)$, is expressed by Boltzmann transport equation:^[41,42]



Scheme 1. Schematic representation of a) Poly(Na₂Ni-ets), b) Poly(Na₂Ni-bts), c) Poly(Na₂Ni-nts), d) Poly(Na₂Ni-ats), e) Poly(Na₂Ni-tts), and f) Poly(Na₂Ni-pts). P_z orbital points in the c-direction. [Color figure can be viewed at wileyonlinelibrary.com]

$$\frac{\partial f}{\partial t} = -\mathbf{v} \cdot \nabla_{\mathbf{r}} f + \frac{e}{\hbar} \left(\mathbf{E} + \frac{1}{c} \mathbf{v} \times \mathbf{H} \right) \cdot \nabla_{\mathbf{k}} f + \left. \frac{\partial f}{\partial t} \right|_{\text{scatt.}} \quad (3)$$

In eq. 3 \mathbf{v} is the group velocity vector as $\mathbf{v} = \frac{1}{\hbar} \nabla_{\mathbf{k}} \varepsilon_{\mathbf{k}}$. The relaxation time τ is the measure of the time required by the electrons to restore to the equilibrium distribution via scatterings. The scattering term is usually simplified by the relaxation time approximation:

$$\left. \frac{\partial f}{\partial t} \right|_{\text{scatt.}} = -\frac{f - f_0}{\tau} \quad (4)$$

The Boltzmann transport equation is a semi-classical equation such as the motion of electrons in solid (more details can be found elsewhere.^[43,44]). This requirement is fulfilled when the size of electronic device is far larger than the unit cell. In addition, the external field should be weak and changing slowly so that the Ehrenfest theorem can be satisfied. These conditions are fulfilled for our MOCP system calculations.

In the presence of a weak electric field and considering only the first-order term, the steady state distribution can be written as

$$f_{\mathbf{k}} = f_0(\varepsilon_{\mathbf{k}}) + e \frac{\partial f_0(\varepsilon_{\mathbf{k}})}{\partial \varepsilon_{\mathbf{k}}} \tau_{\mathbf{k}} \mathbf{v}_{\mathbf{k}} \cdot \mathbf{E} \quad (5)$$

Using the definition of electrical conductivity and Seebeck coefficient, the expression of the former two quantities can be derived as

$$\sigma = e^2 \sum_{\mathbf{k}} \left(-\frac{\partial f_0(\varepsilon_{\mathbf{k}})}{\partial \varepsilon_{\mathbf{k}}} \right) \mathbf{v}_{\mathbf{k}} \mathbf{v}_{\mathbf{k}} \tau_{\mathbf{k}} \quad (6)$$

$$S = \frac{e}{\sigma T} \sum_{\mathbf{k}} \mathbf{v}_{\mathbf{k}} \mathbf{v}_{\mathbf{k}} \tau_{\mathbf{k}} \left(-\frac{\partial f_0(\varepsilon_{\mathbf{k}})}{\partial \varepsilon_{\mathbf{k}}} \right) (\varepsilon_{\mathbf{k}} - \varepsilon_f) \quad (7)$$

Both the conductivity and Seebeck coefficient are tensors, whose components are

$$\sigma_{\alpha\beta} = e^2 \sum_{\mathbf{k}} \left(-\frac{\partial f_0(\varepsilon_{\mathbf{k}})}{\partial \varepsilon_{\mathbf{k}}} \right) v_{\mathbf{k}}^{\alpha} v_{\mathbf{k}}^{\beta} \tau_{\mathbf{k}} \quad (8)$$

$$S_{\alpha\beta} = \frac{e}{\sigma_{\alpha\beta} T} \sum_{\mathbf{k}} v_{\mathbf{k}}^{\alpha} v_{\mathbf{k}}^{\beta} \tau_{\mathbf{k}} \left(-\frac{\partial f_0(\varepsilon_{\mathbf{k}})}{\partial \varepsilon_{\mathbf{k}}} \right) (\varepsilon_{\mathbf{k}} - \mu) \quad (9)$$

respectively.

The charge carrier concentration is defined from above distribution function and the density of state (DOS) $g(\varepsilon)$, for electron and hole, respectively, as follows:

$$N_n = 2 \int_{CB} g(\varepsilon) f^0(\varepsilon_{\mathbf{k}}) d\varepsilon \quad (10)$$

$$N_p = 2 \int_{VB} g(\varepsilon) (1 - f^0(\varepsilon_{\mathbf{k}})) d\varepsilon \quad (11)$$

According to eqs. 8 and 9, the band energies $\varepsilon_{\mathbf{k}}$ on a k-mesh of $8 \times 1 \times 1$ for all the systems were calculated based on the

converged charge density, $\tau(\mathbf{k})$ is relaxation time originating from long wavelength acoustic phonons scattering. Based on deformation potential model, the relaxation time from longitudinal acoustic phonons scatterings can be expressed as:

$$\frac{1}{\tau(\mathbf{k})} = \frac{2\pi k_B T E_1^2}{\hbar C_{ij}} \sum_{\mathbf{k}'} \delta(\varepsilon_{\mathbf{k}} - \varepsilon_{\mathbf{k}'})(1 - \cos\theta) \quad (12)$$

In the above expression C_{ij} and E_1 are the elastic constant and deformation potential constant, respectively. The elastic constant is calculated as the second-order derivative of total energy shift on dilation, the lattice is deformed individually in main chain direction. The deformation potential constant is calculated as the valence (conduction) band energy shift on dilation for hole (electron).^[45-47]

Results and Discussion

Geometric and electronic structures

The crystal structure of heavy Na-doped polymer (two Na ions doping in unit cell) was taken from Ref. ^[29] with one-dimensional periodic boundary conditions, as shown in Scheme 1. All the geometric parameters are listed in Supporting Information Table S1. We found that the MOCPs show good planarity and a very little changes in bond lengths with successive addition of one benzene ring in each system while moving from 0, 1, 2...5 rings system, respectively. Sun et al. found that electrochemical oxidation can modulate the counter Na ions ratio and then carrier concentration.^[21] With respect to pristine and light doped cases (one Na ions doping in unit cell), the geometrical optimization and band structure calculation has been performed, as shown in Supporting Information Figure S3. We found that the sodium doping does not change the band structures and, therefore, rigid band approximation satisfied. And thereby, the doping effect can be modeled simply by shifting the Fermi level position. To simplify the story, we following discuss the band structure based on heavy Na atoms doped cases and assuming Fermi level will be shifted according to the carrier concentration.

The variations in elastic constant can be explained by considering the strength of bonds involved. The C-C covalent bond in an aromatic ring possesses stronger bond than the Ni-S coordinate bond, for the former has much shorter bond length (~1.3 Å) than the latter (~2.3 Å). From $r = 0$ to $r = 5$, the number of stronger C-C bonds per unit length increases, which leads to larger elastic constant. The deformation potential is related to the electronic band structure. For polymers with similar structures, the deformation potential constant is small when the wave function, thus, charge is delocalized along the stretching direction (the direction along the polymer chain here).^[48] For the same system, the charge of flat band is more delocalized than the wide one along the stretching direction. The deformation potential of the flat band maximum (for VB, minimum when it is CB) is smaller, which agrees with our prediction. For the bands with the same type (flat band or wide band here), the charge becomes more localized along the stretching direction as r increases. Hence, the deformation potential constant

increases with r . Both the elastic constant and the deformation potential grow up with the increase of r . These two parts cancel each other when calculating the relaxation time [in accordance with eq. 12].

The electronic band structures, total densities of states DOS, and charge density distribution at the conduction band minimum (CBM) and at the valence band maximum (VBM) for different organic linker are shown in Figure 1. For ethylene organic ligand, the conduction band reveals large dispersion, with wavefunction delocalized on the Se P_z orbitals (P_z orbital is along the c -axis, perpendicular to the NiSe_4 polymer in ab -plane). P_z orbitals of ethylene ligands and the d orbital of Ni, and thus large dispersion for conduction band. While the valence band present flat character, which is comprised of localized d orbital of Ni atom and P_z orbitals of Se atoms.

With organic linker length increasing, the lowest unoccupied molecular orbital (LUMO) energy of organic ligand will shift downwards, the highest occupied molecular orbital (HOMO) energy level will shift upwards with the length of fused acene increase.^[29] The valence band and conduction band undergoes cross over at benzene (bts) and naphthalene (nts), and, thus, $\text{Poly}(\text{Na}_2\text{Ni}(\text{bts}))$, $\text{Poly}(\text{Na}_2\text{Ni}(\text{nts}))$ have no bandgap and reveal metal like properties. When the LUMO energy level shifts downward in further, two bands separated, and thus, the original conduction band turn to the valence band, and the original valence band turn to the conduction band for $\text{Poly}(\text{Na}_2\text{Ni}(\text{ats}))$, $\text{Poly}(\text{Na}_2\text{Ni}(\text{tts}))$, and $\text{Poly}(\text{Na}_2\text{Ni}(\text{pts}))$. Therefore, the conduction band width (CBW) decreases and valence band width (VBW) increases.

For the anthracene, tetracene, and pentacene organic ligands, the conduction band localized to organic ligand mainly, while the valence band delocalized on the d orbital of Ni atom, the P_z orbital of Se atoms, and the P_z orbital of C atoms. Consequently, the density of state (DOS) exhibits a sharp peak near the Fermi level. The valence band shows large dispersion than that of conduction band. Large band dispersion suggests high charge mobility; while sharp DOS distribution promises large Seebeck coefficients. Through engineering band structure and density of states (DOS) to combine large electrical conductivity and large Seebeck, we can thereafter modulate charge transport and TE properties.

Thermoelectric properties

Under the deformation potential approximation, the elastic constant and deformation potential constant can be derived through acoustic phonon scattering at long wavelength limit. Based on Boltzmann transport equation (BTE), we can obtain electrical conductivity σ and Seebeck coefficient S as a function of charge carrier concentration within the rigid band approximation. It has been noted that TE properties are very sensitive to temperature and charge carrier concentrations.^[10,47–49] The rigid band approximation assumes that the doping process can be achieved by shifting the Fermi energy irrespective of the band structure variation. This approximation has been widely adopted in previous theoretical reports about properties of organic TE materials.^[1,10,50–52] Compared with the band structure of intrinsic $\text{Poly}(\text{Ni}(\text{ets}))$ in Supporting Information Figure S3, the zero of

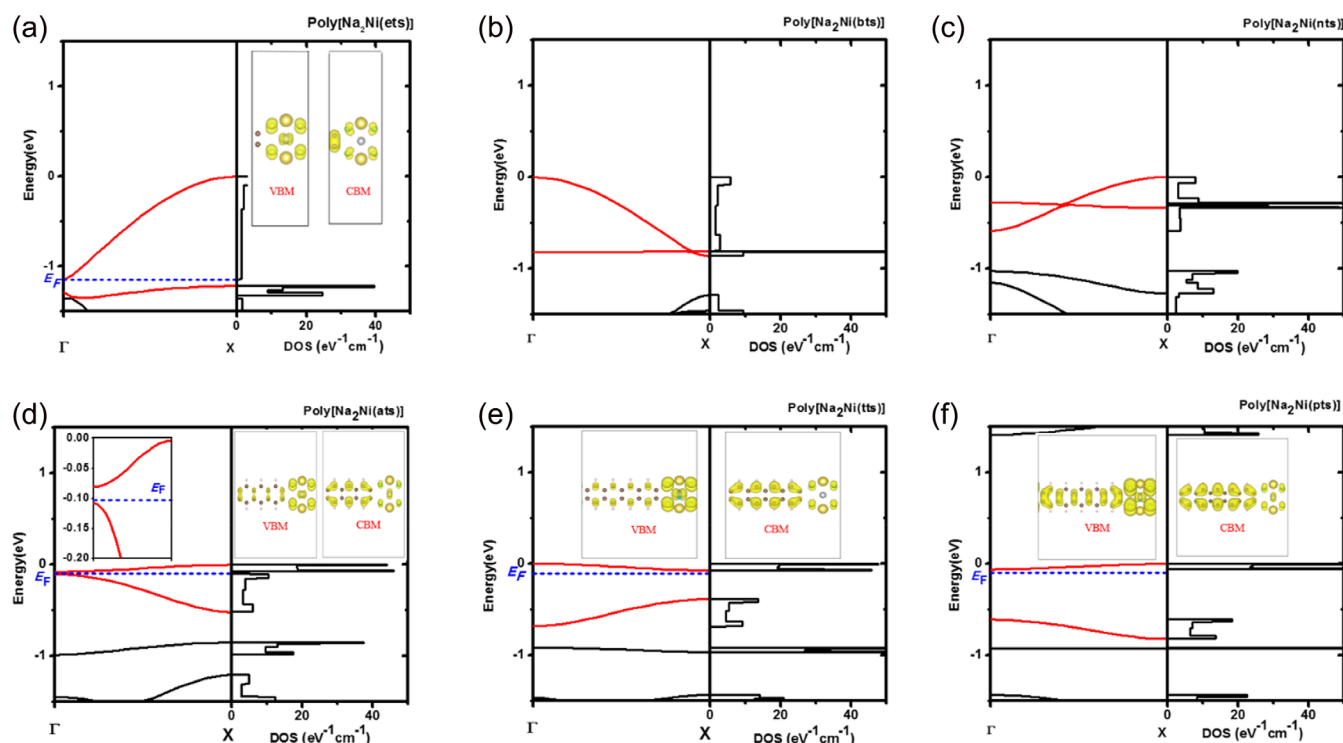


Figure 1. Electronic band structures, total densities of states (DOS), charge density at high symmetry points, that is, Γ and X point for valence band maximum (VBM) and conduction band minimum (CMB) of a) $\text{Poly}(\text{Na}_2\text{Ni}(\text{ets}))$, b) $\text{Poly}(\text{Na}_2\text{Ni}(\text{bts}))$, c) $\text{Poly}(\text{Na}_2\text{Ni}(\text{nts}))$, d) $\text{Poly}(\text{Na}_2\text{Ni}(\text{ats}))$, e) $\text{Poly}(\text{Na}_2\text{Ni}(\text{tts}))$, and f) $\text{Poly}(\text{Na}_2\text{Ni}(\text{pts}))$. The blue dashed line shows the Fermi level corresponding to the best doping concentration at the highest power factor. In part (d) inset plot shows the magnified view of band gap. [Color figure can be viewed at wileyonlinelibrary.com]

Table 1. Thermoelectric parameters: effective mass, carrier concentration, Seebeck coefficients, electrical conductivities, and power factors at 300 K.

MOCPs	Effective mass (m_e^*)		$^{[a]}N(\text{cm}^{-3})$	$S (\mu\text{VK}^{-1})$	$\sigma (\text{Scm}^{-1})$	PF ($\mu\text{Wm}^{-1} \text{K}^{-2}$)
	Electron	hole				
Poly($\text{Na}_2\text{Ni}(\text{ets})$)	0.04	4.50	-1.98×10^4	-128.20	285.01	470
Poly($\text{Na}_2\text{Ni}(\text{ats})$)	0.60	0.27	-5.19×10^5	166.30	531.02	1471
Poly($\text{Na}_2\text{Ni}(\text{tts})$)	0.76	0.23	-1.11×10^6	-200.21	17.90	72
Poly($\text{Na}_2\text{Ni}(\text{pts})$)	0.74	0.22	-9.20×10^5	-204.01	18.20	76

[a] Carrier Concentration defined in BoltzTraP code as $N = N_p - N_n$

energy for Poly($\text{Na}_2\text{Ni}(\text{ets})$) corresponds to the top of the conduction band, as shown in Figure 1, which mean counter ions two Na^+ in one unit cell corresponds to high electron concentration doping. Different counter ions concentration and oxidation will induce different carrier concentration. Here, we present the optimal carrier concentration to maximize the power factor, the Fermi energy (E_F) is shifted and labeled as blue line as show in Figure 1. Under the concentration of $-1.98 \times 10^4 \text{ cm}^{-3}$, the Poly (Ni(ets)) is calculated with the maximum power factor of $470 \mu\text{Wm}^{-1} \text{K}^{-2}$ at room temperature (300 K), as shown in Table 1. Due to high electrical conductivity and relatively large Seebeck coefficient, the Poly($\text{Na}_2\text{Ni}(\text{ets})$) show the largest power factor among all N-type compounds.

In the case of organic ligands containing benzene and naphthalene for Poly($\text{Na}_2\text{Ni}(\text{bts})$) and Poly($\text{Na}_2\text{Ni}(\text{nts})$); these two systems, having no bandgap and metal like properties, will go against to TE properties, and thus we don't discuss them in this work. With respect to anthracene (ats) organic ligand, the band gap becomes significantly narrow in this condition. When the Fermi level is close to the crossing point between the valence and the conduction band, both the wide band and the flat band contribute to the transport. The transport function $\sigma(E) = eN(E)\mu(E)k_B T$ (by Mott and Cutler^[53]) is determined by $N(E)$ the density of states, and $\mu(E)$ the energy-dependent carrier mobility, which have a sudden change at the crossing point (or at the band edge). the final sign of Seebeck coefficient can be understood by the following expression:^[54]

$$S = -\frac{1}{\sigma} \left(\frac{k_B}{e} \right) \int \left(\frac{E - E_F}{k_B T} \right) \sigma(E) \left(-\frac{\partial f}{\partial E} \right) dE \quad (13)$$

Since the Seebeck coefficient is sensitive to $(E - E_F)$ as well as the distribution of $N(E)$ and $\mu(E)$. Flat band has higher $N(E)$ but lower $\mu(E)$, while the wide band has higher $\mu(E)$ but lower $N(E)$. Because the Poly($\text{Na}_2\text{Ni}(\text{ats})$) presents opposite character for valence and conduction band, as shown in Figure 1d, the holes in valence band have larger $\sigma(E)$ than the electrons, and, thus, this system reveal overall positive and the largest Seebeck coefficient for investigated systems. Combined with moderate electrical conductivity, Poly($\text{Na}_2\text{Ni}(\text{ats})$) possesses the highest P-type Power Factor of $1471 \mu\text{Wm}^{-1} \text{K}^{-2}$ at 300 K.

In the case of tetracene and pentacene organic ligands, the Fermi energy level lies in flat conduction bands, which is far from the valence band due to large bandgap. The TE properties can be analyzed in the frame of a one-band model. The expression for Seebeck Coefficient can be simplified as follows according to Sommerfeld expansion:

$$S \approx -\frac{\pi^2 k_B^2 T}{3e} \frac{d \ln \sigma(E)}{dE} \Big|_{E=E_F} \quad (14)$$

Here, $\sigma(E)$ can be expand to $\sigma(E) = eN(E)\mu(E)k_B T$,^[53] $N(E)$ is the density of states, and $\mu(E)$ is the energy-dependent carrier mobility. Bubnova et al.^[52] has pointed out that the change of $\mu(E)$ is trivial and then $S \propto d \ln N(E) / dE|_{E=E_F}$. Here, $d \ln N(E) / dE|_{E=E_F} > 0$, considering the flat conduction band induce low conductivity for electron, and thus Poly($\text{Na}_2\text{Ni}(\text{tts})$) and Poly($\text{Na}_2\text{Ni}(\text{pts})$) possesses moderate power factor act as an N-type organic TE material. Similar band structure and effective mass induce similar TE properties for Poly($\text{Na}_2\text{Ni}(\text{tts})$) and Poly($\text{Na}_2\text{Ni}(\text{pts})$).

To investigate the relationship of thermoelectric properties with doping concentration, we investigated the dependence of electrical conductivity, Seebeck coefficient, and power factor with carrier concentration, as shown in Figure 2. As for the counter ion Na^+ in general induce electron doping, we put emphasis on negative carrier concentration. We found that Poly($\text{Na}_2\text{Ni}(\text{tts})$) Poly($\text{Na}_2\text{Ni}(\text{pts})$) reveal typical semiconductor properties. Similar band structure and effective mass lead to similar TE properties. The Seebeck coefficient drops drastically with carrier concentration. Due to low electrical conductivity for electron, Poly($\text{Na}_2\text{Ni}(\text{pts})$) have relatively low power factor. If hole carrier concentration can be introduced, high conductivity and moderate Seebeck coefficient for hole will suggest high P-type power factor.

Compared with Poly($\text{Na}_2\text{Ni}(\text{tts})$) and Poly($\text{Na}_2\text{Ni}(\text{pts})$), it must be noted that Poly($\text{Na}_2\text{Ni}(\text{ets})$) and Poly($\text{Na}_2\text{Ni}(\text{ats})$) display completely different TE properties dependence on carrier concentration, since these two systems possess very small band gap 80 meV and 27 meV, respectively. The small band gap leads to the coexistence of electrons and holes. This, however, enhances the electrical conductivity but lowers Seebeck coefficient, as here the "zero" carrier concentration does not mean no carriers, but the balance of electron and hole concentration. Due to the large difference in electron and hole band structure and then effective mass, as shown in Table 1. However, the Sofo model supposed similar effective mass for electron and hole should be satisfied.^[55] In this case, Seebeck coefficient will decay to zero at low carrier concentration for narrow band gap system. Due to the large difference in effective mass and then mobility $\mu(E)$ and conductivity $\sigma(E)$ for electron and hole, the Seebeck coefficient does not decay to zero according to eq. 13 at low concentration for narrow bandgap case, the Sofo's model fails in such cases. It should be noted that Poly($\text{Na}_2\text{Ni}(\text{ets})$) display not only high conductivity but also large negative Seebeck coefficient at low carrier concentration, which makes Poly($\text{Na}_2\text{Ni}(\text{ets})$) an excellent N-type thermoelectric material. As

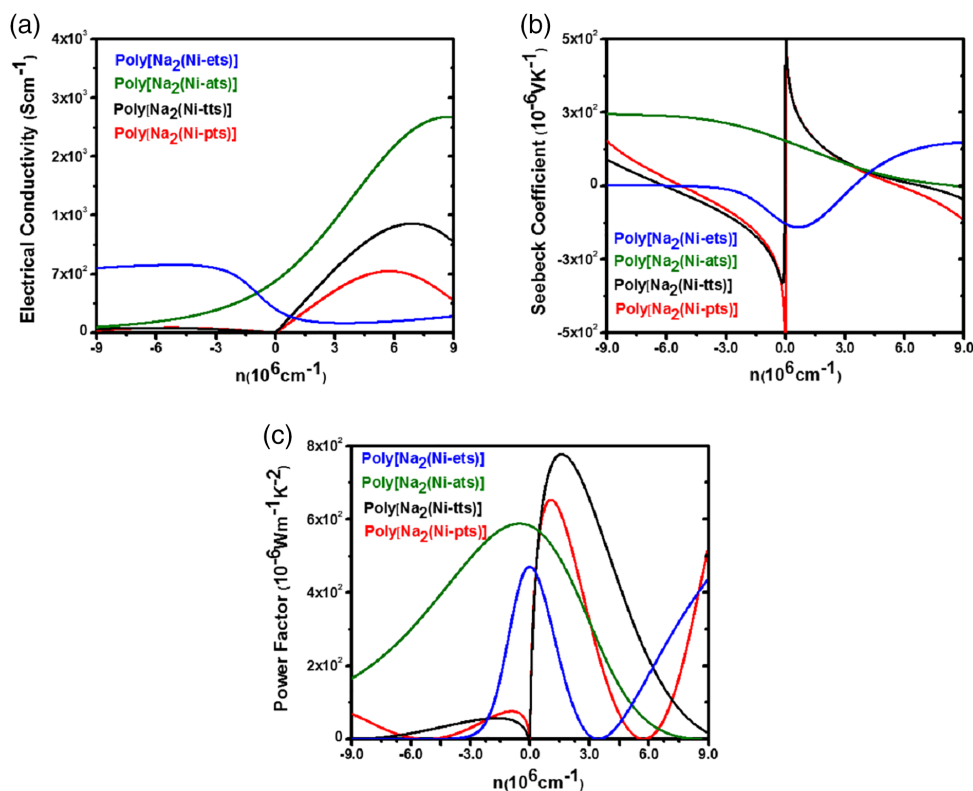


Figure 2. Carrier Concentration dependence of thermoelectric parameters a) electrical conductivity, b) Seebeck coefficient, and c) power factor for Poly(Na₂Ni-ets), Poly(Na₂Ni-ats), Poly(Na₂Ni-tts), and Poly(Na₂Ni-pts). [Color figure can be viewed at wileyonlinelibrary.com]

for Poly(Na₂Ni-ets), the system display wide conduction band and flat valence band and narrow bandgap. However, Poly(Na₂Ni-ats) reveal wide valence band and flat conduction band, the Seebeck coefficient turned positive sign, and high P-type TE properties for Poly(Na₂Ni-ats) can be expected.

To see whether constant relaxation time approximation is applicable or not, we have tested our MOCP systems by plotting relaxation time versus carrier concentration. The results show that the relaxation time converges at high carrier concentration for conduction band (electrons as carriers) and the valence band (holes as carriers) in poly(Na₂Ni(ets)). The constant relaxation time approximation is, therefore, valid for CB and VB in this system.

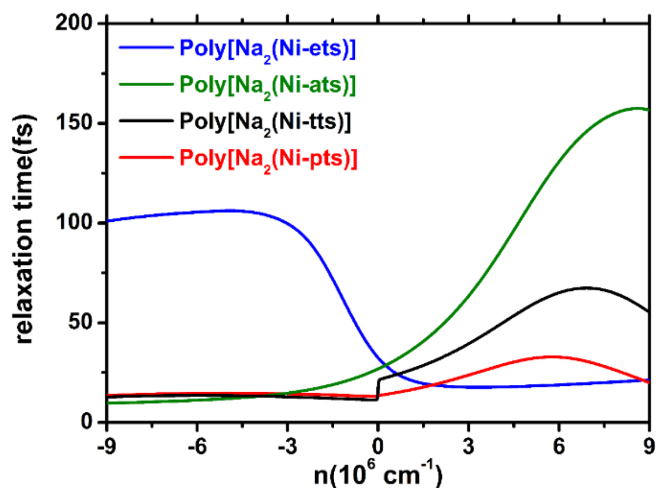


Figure 3. Carrier Concentration vs relaxation time for Poly(Na₂Ni-ets), Poly(Na₂Ni-ats), Poly(Na₂Ni-tts), and Poly(Na₂Ni-pts). [Color figure can be viewed at wileyonlinelibrary.com]

The relaxation time of the valence bands changes much when increasing the carrier concentration except for poly(Na₂Ni(ets)), indicating that $\tau(k)$ varies for different k points (Fig. 3). Hence, the constant relaxation time approximation is not appropriate for the systems, that is, Poly(Na₂Ni-ats), Poly(Na₂Ni-tts), and Poly(Na₂Ni-pts). As a result, it is necessary to use deformation potential theory to obtain k dependent relaxation time instead of constant relaxation time approximation. The reason behind this is not clear and might be discussed in near future work.

Summary and Outlook

In summary, we have investigated the electronic structures and thermoelectric properties of a series of organic MOCPs based on first principles calculations. By introducing different organic linkers with various chain lengths between two inorganic units, the band structures display semiconductor, metal, and finally back again to semiconductor character, because of the relative alignment of the energy level between the d orbital of Ni and π orbitals of acene. The TE properties vary significantly from the N-type to P-type: the Poly(nickel-ethylenetetraselenolate) [Poly(Ni-ets)] material reveal the largest N-type TE alloy properties. With increase in the length of organic linker, Poly(Na₂Ni-ats) presents the largest p-type power factor up to 1471 $\mu\text{Wm}^{-1} \text{K}^{-2}$ at 300 K, which is the highest efficiency ever reported for p-type organic TE materials. This is because of the high carrier concentration resulting from small band gap, suggesting high electrical conductivity. In addition, the large difference in effective masses between conduction band and valence band leads to large Seebeck coefficient. With the bandgap increases, the bandwidth of the conduction band turns narrower with less dispersion for the

acene part, sharpening the DOS distribution for CBM, leading to large negative Seebeck coefficient, and making Poly(Na₂Ni-pts) and Poly(Na₂Ni-tts) efficient n-type TE materials. We conclude that MOCPs have great potential in TE application.

Acknowledgments

ZS is in debt to Professor Qianer Zhang for his strong encouragement. In the occasion of his 90th birthday celebration, ZS sincerely wishes Prof. Zhang great health and longevity. This work is supported by the National Natural Science Foundation of China through CELMA Grant Number 21788102 and Grant Number 21673247, and the National Key R&D Program of China (2017YFA0204700) and Beijing Capacity Building for Sci-Tech Innovation-Fundamental Scientific Research Funds (025185305000), the Chinese Scholarship Council (CSC) and the Strategic Priority Research Program of the Chinese Academy of Sciences (Grant No. XDB12020200). The numerical computation has been carried out in the Tsinghua University High Performance Computing Centre.

Conflict of Interest

There are no conflict of interests to declare.

Keywords: thermoelectric materials · metal organic coordination polymers · Boltzmann-transport-theory · band engineering

How to cite this article: J. Khan, Y. Liu, T. Zhao, H. Geng, W. Xu, Z. Shuai. *J. Comput. Chem.* **2018**, 39, 2582–2588. DOI: 10.1002/jcc.25639



Additional Supporting Information may be found in the online version of this article.

- [1] D. Wang, W. Shi, J. Chen, J. Xi, Z. Shuai, *Phys. Chem. Chem. Phys.* **2012**, 14, 16505.
- [2] R. Fei, A. Faghaninia, R. Soklaski, J. A. Yan, C. Lo, L. Yang, *Nano Lett.* **2014**, 14, 6393.
- [3] R. Kroon, D. A. Mengistie, D. Kiefer, J. Hynynen, J. D. Ryan, L. Yu, C. Müller, *Chem. Soc. Rev.* **2016**, 45, 6147.
- [4] C. Gayner, K. K. Kar, *Prog. Mater. Sci.* **2016**, 83, 330.
- [5] N. Mateeva, H. Niculescu, J. Schlenoff, L. R. Testardi, *J. Appl. Phys.* **1998**, 83, 3111.
- [6] D. Huang, Y. Zou, F. Jiao, F. Zhang, Y. Zang, C. A. Di, W. Xu, D. Zhu, *ACS Appl. Mater. Interfaces* **2015**, 7, 8968.
- [7] Y. Sun, J. Zhang, L. Liu, Y. Qin, Y. Sun, W. Xu, D. Zhu, *Sci. China Chem.* **2016**, 59, 1323.
- [8] Q. Zhang, Y. Sun, W. Xu, D. Zhu, *Adv. Mater.* **2014**, 26, 6829.
- [9] Y. Jiang, H. Geng, W. Shi, Q. Peng, X. Zheng, Z. Shuai, *J. Phys. Chem. Lett.* **2014**, 5, 2267.
- [10] W. Shi, J. Chen, J. Xi, D. Wang, Z. Shuai, *Chem. Mater.* **2014**, 26, 2669.
- [11] C. A. Di, W. Xu, D. Zhu, *Natl. Sci. Rev.* **2016**, 3, 269.
- [12] G. Tan, L. D. Zhao, M. G. Kanatzidis, *Chem. Rev.* **2016**, 116, 12123.
- [13] G.-H. Kim, L. Shao, K. Zhang, K. P. Pipe, *Nat. Mater.* **2013**, 12, 719.
- [14] O. Bubnova, Z. U. Khan, A. Malti, S. Braun, M. Fahlman, M. Berggren, X. Crispin, *Nat. Mater.* **2011**, 10, 429.
- [15] N. E. Coates, S. K. Yee, B. McCulloch, K. C. See, A. Majumdar, R. A. Segalman, J. J. Urban, *Adv. Mater.* **2013**, 25, 1629.
- [16] R. Yue, J. Xu, *Synth. Met.* **2012**, 162, 912.
- [17] W. Shi, T. Zhao, J. Xi, D. Wang, Z. Shuai, *J. Am. Chem. Soc.* **2015**, 137, 12929.
- [18] W. Li, S. Lin, X. Zhang, Z. Chen, X. Xu, Y. Pei, *Chem. Mater.* **2016**, 28, 6227.
- [19] W. G. Zeier, A. Zevalkink, Z. M. Gibbs, G. Hautier, M. G. Kanatzidis, G. J. Snyder, *Angew. Chem. Int. Ed.* **2016**, 55, 6826.
- [20] M. He, J. Ge, Z. Lin, X. Feng, X. Wang, H. Lu, Y. Yang, F. Qiu, *Energy Environ. Sci.* **2012**, 5, 8351.
- [21] Y. Sun, L. Qiu, L. Tang, H. Geng, H. Wang, F. Zhang, D. Huang, W. Xu, P. Yue, Y. S. Guan, F. Jiao, Y. Sun, D. Tang, C. A. Di, Y. Yi, D. Zhu, *Adv. Mater.* **2016**, 28, 3351.
- [22] H. Poleschner, W. John, F. Hoppe, E. Fanghxnell, S. Roth, *J. für Prakt. Chem.* **1983**, 51, 11.
- [23] A. K. Menon, E. Uzunlar, R. M. W. Wolfe, J. R. Reynolds, S. R. Marder, S. K. Yee, *J. Appl. Polym. Sci.* **2017**, 134, 44402.
- [24] N. M. Rivera, E. M. Engler, R. R. Schumaker, *J. Chem. Soc. Chem. Commun.* **1979**, 0, 184.
- [25] Y. Tang, X. Gan, M. Tan, X. Zheng, *Synth. Met.* **1998**, 97, 43.
- [26] S. Dahm, D. Schweitzer, *Synth. Met.* **1993**, 57, 884.
- [27] J. R. Reynolds, C. A. Jolly, S. Krichene, P. Cassoux, C. Faulmann, *Synth. Met.* **1989**, 31, 109.
- [28] J. Ramos, *Synth. Met.* **1997**, 86, 1807.
- [29] D. Tiana, C. H. Hendon, A. Walsh, T. P. Vaid, *Phys. Chem. Chem. Phys.* **2014**, 16, 14463.
- [30] Y. Pei, H. Wang, G. J. Snyder, *Adv. Mater.* **2012**, 24, 6125.
- [31] W. Li, S. Lin, B. Ge, J. Yang, W. Zhang, Y. Pei, *Adv. Sci.* **2016**, 3, 1600196.
- [32] H. Wang, Z. M. Gibbs, Y. Takagiwa, G. J. Snyder, *Energy Environ. Sci.* **2014**, 7, 804.
- [33] Y. Pei, X. Shi, A. LaLonde, H. Wang, L. Chen, G. J. Snyder, *Nature* **2011**, 473, 66.
- [34] K. Biswas, J. He, I. D. Blum, C.-I. Wu, T. P. Hogan, D. N. Seidman, V. P. Dravid, M. G. Kanatzidis, *Nature* **2012**, 489, 414.
- [35] G. Kresse, J. Furthmüller, *Comput. Mater. Sci.* **1996**, 6, 15.
- [36] G. Kresse, J. Furthmüller, *Phys. Rev. B* **1996**, 54, 11169.
- [37] J. P. Perdew, M. E. Burke, *Phys. Rev. Lett.* **1996**, 77, 3865.
- [38] J. D. Pack, H. J. Monkhorst, *Phys. Rev. B* **1977**, 16, 1748.
- [39] J. Heyd, G. E. Scuseria, M. Ernzerhof, *J. Chem. Phys.* **2003**, 118, 8207.
- [40] G. K. H. Madsen, D. J. Singh, *Comput. Phys. Commun.* **2006**, 175, 67.
- [41] B. R. Nag, *Electron Transport in Compound Semiconductors*, Springer-Verlag, Berlin, New York, **1980**.
- [42] T. J. Scheidemantel, C. Ambrosch-Draxl, T. Thonhauser, J. V. Badding, J. O. Sofo, *Phys. Rev. B* **2003**, 68, 125210.
- [43] J. M. Ziman, *Principles of The Theory of Solids*, New York (NY) USA: Cambridge University Press, **1972**.
- [44] Y. M. Galperin, *Introduction to Modern Solid State Physics*, Colorado Springs: CreateSpace Independent Publishing Platform, **2014**.
- [45] J. Bardeen, W. Shockley, *Phys. Rev.* **1950**, 80, 72.
- [46] J. Xi, M. Long, L. Tang, D. Wang, Z. Shuai, *Nanoscale* **2012**, 4, 4348.
- [47] T. Zhao, D. Wang, Z. Shuai, *Synth. Met.* **2017**, 225, 108.
- [48] D. Wang, L. Tang, M. Long, Z. Shuai, *J. Chem. Phys.* **2009**, 131, 1.
- [49] Y. Pei, A. D. LaLonde, H. Wang, G. J. Snyder, *Energy Environ. Sci.* **2012**, 5, 7963.
- [50] G. Nan, X. Yang, L. Wang, Z. Shuai, Y. Zhao, *Phys. Rev. B Condens. Matter Mater. Phys.* **2009**, 79, 115203.
- [51] J. Chen, D. Wang, Z. Shuai, *J. Chem. Theory Comput.* **2012**, 8, 3338.
- [52] O. Bubnova, Z. U. Khan, H. Wang, S. Braun, D. R. Evans, M. Fabretto, P. Hojati-Talemi, D. Dagnelund, J. B. Arlin, Y. H. Geerts, S. Desbief, D. W. Breiby, J. W. Andreasen, R. Lazzaroni, W. M. Chen, I. Zozoulenko, M. Fahlman, P. J. Murphy, M. Berggren, X. Crispin, *Nat. Mater.* **2014**, 13, 190.
- [53] M. Cutler, N. F. Mott, *Phys. Rev.* **1969**, 181, 1266.
- [54] S. D. Kang, G. J. Snyder, *Nat. Mater.* **2017**, 16, 252.
- [55] J. O. Sofo, G. D. Mahan, *Phys. Rev. B* **1994**, 49, 4565.

Received: 29 June 2018

Revised: 10 September 2018

Accepted: 13 September 2018

Published online on 15 November 2018